Design, Analysis, and Performance Improvement of the HPM Oscillator Reltron

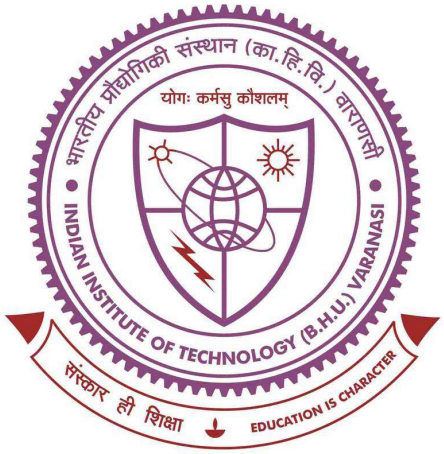

Thesis submitted in partial fulfillment
for the Award of Degree

Doctor of Philosophy

by

Soumojit Shee

DEPARTMENT OF ELECTRONICS ENGINEERING
INDIAN INSTITUTE OF TECHNOLOGY
(BANARAS HINDU UNIVERSITY)
VARANASI – 221 005

ROLL NO: 17091027 **2020**

CHAPTER 6

Summary, Conclusion and Future scope

6.1 Introduction

Reltron's simple construction, inexpensive and elementary cathode technology, and easy power extraction bring a number of attributes and make it an outstanding device. It combines the working principles and qualities of two devices, the SCO and the biased gap klystron. The EM field distribution in reltron's operating normal mode is similar to that of the SCO's, and the postacceleration of the bunched beam is similar to the biased gap klystron's. Many apparent features (discussed in section 2.4), which occur quite naturally in the reltrons, are rather difficult to achieve in other HPM sources. Motivated by the prospects, further work has been carried out and reported in the present dissertation. This includes; i) perceiving the interconnection among the normal modes and the structural parameters of modulation section, ii) extending the dispersion relation of a side-coupled LINAC to that of a reltron, and calculating the structure-specific coupling coefficient between the on-axis cavities and the side coupling cavity, iii) investigating the performance when some relevant parameters of the RF interaction structure are varied, and iv) exploring new possible characteristics when the number of side cavities is increased.

The present chapter summarizes the studies carried out in the previous chapters and points out the limitations of the present study.

6.2 Summary and Conclusion

6.2.1 Chapter 1

Introduction and Literature Review: In this chapter, the three fundamental types of radiation mechanisms are introduced at the beginning. The origin of HPM technology and the historical advancement of various HPM sources are discussed to trace the technology development trends. A detailed review of the available literature has been carried out to comprehend the device and make a state-of-the-art table (Table 1.1 in Chapter 1). This also helped to find out some of the research gaps as follows;

(i) ambiguous relation among the normal modes and the dimensional parameters,

(ii) the dispersion relation of the RF interaction structure is not outlined,

(iii) the effects of modulation section parameters on performance, and tunability,

(iv) the possibility of performance improvement with more numbers of side cavities.

A course of action has been decided to address those points, and the successive chapters are planned accordingly.

6.2.2 Chapter 2

Parametric Study of Normal Mode Frequencies and Cold-test Results: This chapter is dedicated to bridge the research gap (i). The reltron sub-assemblies and their working principle are presented at the beginning, followed by the collection of features. The EM field patterns and frequencies of the normal modes are obtained next, and mode designations are explained along with the Eigenmode solver of CST-MWS and MAGIC. The two software packages have been used for cross-validating the simulation results. The obtained EM field patterns in the three lower-order normal modes matched in both the solvers and substantial matching have been obtained between the mode frequencies. This difference in frequency resulted from different meshing techniques of FIT based CST-MWS and FDTD based MAGIC. However, a closer frequency match has been found between two solvers (Eigenmode and Frequency domain) of CST-MWS.

The MAGIC code failed to obtain mode '0' in earlier work. To successfully capture all the three modes, a full 3D cavity structure is modeled instead of considering the axial symmetry. The apparent axial symmetry is misleading as the side cavity is asymmetric along the azimuth. Also, a narrower window was set, and the range of frequency was specified in the MAGIC code with prior knowledge from CST-MWS. This set-up has captured all three modes.

For parametric study of normal mode frequencies, the mode frequencies are recorded in the post-processing window, while the dimensional parameters are varied sequentially. The variations are kept within respective ranges, which modifies the mode frequencies considerably, and does not alter the order of their occurrence. Thus, the dependence of mode frequencies on the dimensional parameters is established. The study concludes that three parameters govern the frequency and mode separation. The main cavity radius (*r_mc*) dominantly governs the operating frequency, and the coupling depth (*d*) makes minor adjustment. The idler disc length (l_idl) is the one that governs both- mode separation as well as operating frequency.

The parametric study results are valid for all frequency bands as the frequency, and the cavity dimensions are scalable. During the process of the parametric study, the cavity dimensions are optimized for equal and maximum separation between the three modes. Though the normal mode frequencies can accurately be predicted by simulation, they can not be measured directly.

To calculate the quality factors and the cavity reactance in all three modes, the S_{11} is simulated by using the Frequency-domain solver. The calculated parameters are important for taking the beam loading into consideration. The methods of the frequency domain solver are also discussed briefly.

The frequencies of S_{11} minima are found to coincide with that of the normal modes with less than 0.2% variation. This aids in an indirect measurement of the normal mode frequencies. To measure the S_{11}, a modulation section is constructed with the previously optimized cavity dimensions from an electrical grade copper sheet. The simulated and measured frequencies of S_{11} minima matched with the good agreement, considering the

human error involved in constructing the test-cavity parts and the subsequent difference between the assembled cavity and the ideal simulation model. The difference in the dB level between the experimental and the simulated result is due to losses in the practical measurement set-up. The measured result indicates that waves with a frequency near the operating mode $\pi/2$ traverse the structure with the least reflection than the other two. The construction of the modulation section, measurement set-up, and the measured results have been discussed in detail.

6.2.3 Chapter 3

Electromagnetic Analysis: The electromagnetic analysis leading to the dispersion relation of reltron's RF interaction structure has been discussed here, which addresses the research gap (ii). The equivalent circuit model of the cavity resonator has been used. The matrix method is used to solve the circuit equations, which are formed and rearranged as an eigenvalue problem. The solutions give the eigenvalues (oscillation frequencies) and the corresponding eigenvectors (relative direction of currents). The dispersion relation has been derived thereafter from the generalized eigenvalue equations. Numerical simulations have been carried out to find the eigenvalues and the corresponding eigenvectors at different coupling depths. The coupling coefficient, specific to the designed modulation section has been calculated.

As the reltron's modulation section consists of three cavities, and it supports three normal modes. The frequency differences among these modes are not equal, in general, because of the nonlinear relation between the frequency and the coupling coefficient. Proper tuning is necessary for optimum performance.

The increase in mode separation with coupling depth matched with the analytical result. The coupling coefficient increases monotonically as the coupling depth increases. The resonant frequency of the on-axis cavities decreases, while that of the coupling cavity remains relatively constant.

6.2.4 Chapter 4

PIC Simulation and Result: This chapter describes the simulation results of an S-band reltron and thereby addresses the research gap (iii). A way of setting up the simulation for reproducing the original experimental work has been discussed here.

The obtained output frequency from PIC solver is found to be closest to the $\pi/2$ mode frequency predicted by Eigenmode solver. This confirms only $\pi/2$ mode transfers net energy from the beam to the field.

The reduction in the output frequency than the cold frequency reveals the effect of beam loading. FT of the output signal is relatively monotonous in comparison to VIRCATOR and RM as the interaction with 0, and π modes do not play any role in beam bunching. Unwanted mode jumping, as well as frequency chirping, is not found.

Increasing the mode separation (by tuning the idler disc) shows improvement in the output power and efficiency up to a critical level accompanied by a down-shift in frequency, resulting from the declining $\pi/2$ mode. An increase beyond this point cuts down both the output power and efficiency. When mode separation is further increased, the pulse duration reduces substantially with a subsequent reduction in energy per pulse.

The effect of coupling depth d on device performance has also been studied (Table 4.3).

The phase-space plot provides important insight into the device operation, and it also shows the decrease in energy spread due to the application of post-acceleration potential. The reduction in energy spread with the application of post acceleration potential has been shown using the phase space plot.

The range of frequency tunability achievable through tuning three of the relevant cavity parameters has also been demonstrated.

6.2.5 Chapter 5

Performance Improvement: This presents the performance improvement study of the existing device, addressing the research gap (iv). Double, triple, and quad side-cavity reltrons have been explored through simulation. However, only the double side-cavity (DSC)

reltron has demonstrated performance improvement in terms of the faster start-up of oscillation, which leads to prolonged pulse duration and higher energy per pulse. Simulation results predicted that the dual cavity extraction section could be successfully utilized in this kind of reltron, as well. Beam-absent, beam-present, and electrostatic simulations have been performed. In addition to the three normal modes in a conventional reltron, an extra mode (pseudo $\pi/2$ mode) has been identified in the DSC reltron. The performance chart of the proposed device has been obtained in terms of output power and efficiency.

Four normal modes appear in a DSC reltron modulation section, as it is comprised of four cavities. The Eigenmode solver has successfully captured all four modes. The pseudo $\pi/2$ mode has zero electric field at the cavity axis and minimum at its surroundings. Hence, it does not interfere with the beam wave interaction process.

Here also, the operating frequency is found to be closest to that of $\pi/2$ mode, confirming the $\pi/2$ mode operation. The spectrum does not show any evidence of mode hopping or frequency chirping as the conventional reltron. However, the operating frequency is $\sim$43 MHz lower than the $\pi/2$ mode frequency that shows the effect of beam loading, which is common in all vacuum electron devices.

A significant amount of power has been contained by the second harmonics, which would increase the effectiveness of reltron as a DEW.

The efficiency of the DSC reltron without applied postacceleration potential is found to be 20%, which is the same as the conventional reltron experiments. The reduction in efficiency at higher applied postacceleration potential might be due to the difficulty in beam bunching at relativistic velocities.

The result of the Electrostatic solver clarified that the increase in beam current with the postacceleration potential is due to the raised static electric field at the AK-gap.

More than two cavities can be used for microwave extraction. However, the phase difference between the respective port signals becomes considerable when more than two consecutive cavities are considered, resulting in reduced output power.

In the final conclusion, reltron has a collection of exceptional qualities, which are desirable in an HPM device. The design, analysis, and performance improvement have been

discussed. The author hopes his modest effort in the form of this dissertation will be helpful for better understanding and future improvement of reltron.

6.3 Limitation of Present Work and Further Scope

- The reltrons reportedly used solid beams either from a cold cathode or from a thermionic cathode. So, the solid pencil beams have been adopted in all the present studies. However, the annular beams can carry a higher current than a solid beam at the same given voltage. Primary simulations with annular beams have shown promising results. Further study of hollow beam reltrons is recommended.

- The extraction section can be extended to more than two cavities, and the power can be combined with an additional power combiner, treading the compactness.

- Phase locking of multiple could be achieved, as demonstrated by RMs and SCOs.

- The calculated cavity reactance in each mode may be extended for a detailed analytical study of beam loading, which is evident from the downshift of oscillation frequency with respect to the cold frequency.

- The cathode technology has taken a big leap in recent years. The new generation of nano-structure based cathodes is capable of delivering much higher emission density. If this may be translated to the high power domain to make the use of IREB technology, microwave tubes, including reltrons, may reach new heights.